Phys. Eng. Sci. Med. manuscript No.
(will be inserted by the editor)

Dosimetric evaluation of a patient-specific 3D-printed oral positioning stent for head-and-neck radiotherapy

Susannah Cleland* · **Philip Chan** · **Benjamin Chua** · **Scott B. Crowe** · **Jodi Dawes** · **Lizbeth Kenny** · **Charles Lin** · **Elise Obereigner** · **Samuel C. Peet** · **Jamie V. Trapp** · **Tania Tutaki** · **Tanya Kairn**

the date of receipt and acceptance should be inserted later

* Present address: Radiation Oncology Princess Alexandra Hospital Raymond Terrace, South Brisbane, QLD 4101, Australia.

Susannah Cleland
Royal Brisbane and Women's Hospital, Herston, QLD 4029, Australia, and
Queensland University of Technology, Brisbane, QLD 4001, Australia, and
Herston Bifabrication Institute, Metro North Hospital and Health Service, Herston QLD 4029, Australia

Philip Chan, Jodi Dawes, Charles Lin
Royal Brisbane and Women's Hospital, Herston, QLD 4029, Australia

Benjamin Chua, Lizbeth Kenny
Royal Brisbane and Women's Hospital, Herston, QLD 4029, Australia, and
University of Queensland, Brisbane, QLD 4072, Australia

Elise Obereigner, Tania Tutaki
Royal Brisbane and Women's Hospital, Herston, QLD 4029, Australia, and
Herston Bifabrication Institute, Metro North Hospital and Health Service, Herston QLD 4029, Australia

Samuel C. Peet
Royal Brisbane and Women's Hospital, Herston, QLD 4029, Australia, and
Queensland University of Technology, Brisbane, QLD 4001, Australia

Jamie V. Trapp
Queensland University of Technology, Brisbane, QLD 4001, Australia

Scott B. Crowe, Tanya Kairn
Royal Brisbane and Women's Hospital, Herston, QLD 4029, Australia, and
Queensland University of Technology, Brisbane, QLD 4001, Australia, and
Herston Bifabrication Institute, Metro North Hospital and Health Service, Herston QLD 4029, Australia, and
University of Queensland, Brisbane, QLD 4072, Australia
E-mail: t.kairn@gmail.com

Abstract As head-and-neck radiotherapy treatments become more complex and sophisticated, and the need to control and stabilise the positioning of intra-oral anatomy therefore becomes more important, leading the increasing use of oral positioning stents during head-and-neck radiotherapy simulation and delivery. As an alternative to the established practice of creating oral positioning stents using wax, this study investigated the use of a 3D printing technique. An Ender 5 3D printer (Creality 3D, Shenzhen, China) was used, with PLA+ "food-safe" polylactic acid filament (3D Fillies, Dandenong South, Australia), to produce a low-density 3D printed duplicate of a conventional wax stent. The physical and dosimetric effects of the two stents were evaluated using radiochromic film in a solid head phantom that was modified to include flexible parts. The Varian Eclipse treatment planning system (Varian Medical Systems, Palo Alto, USA) was used to calculate the dose from two different head-and-neck treatment plans for the phantom with each of the two stents. Examination of the resulting four dose distributions showed that both stents effectively pushed sensitive oral tissues away from the treatment targets, even though most of the phantom was solid. Film measurements confirmed the accuracy of the dose calculations from the treatment planning system, despite the steep density gradients in the treated volume, and demonstrated that the 3D print could be a suitable replacement for the wax stent. This study demonstrated a useful method for dosimetrically testing novel oral positioning stents. We recommend the development of flexible phantoms for future studies.

Keywords Radiation therapy · additive manufacture · rapid prototyping · dosimetry

1 Introduction

A wide range of head-and-neck cancers can be treated effectively using sophisticated radiotherapy techniques [1–6], especially when suitable patient positioning and immobilisation is achieved [7–9]. In particular, the use of modulated radiotherapy techniques, such as intensity modulated radiotherapy (IMRT) and volumetric modulated arc therapy (VMAT or IMAT) can allow very conformal doses of radiation to be delivered to treatment targets, while minimising doses to the many surrounding sensitive organs and tissues in the head-and-neck region [1–3], provided that the effected tissues can be positioned reproducibly in relation to the radiation beams [7–11].

The use of external immobilisation equipment (head-rests, vac-bags, thermoplastic masks or shells) to achieve stable and reproducible positioning of the head and neck is well established [7–11]. Due to the precise patient positioning needed to accurately deliver the complex dose distributions achievable using modulated radiotherapy techniques, the importance of achieving stable and reproducible positioning of the finer, more-mobile anatomical structures in this region (lips, cheeks, tongue) is increasingly being recognised [12–16].

Customised intra-oral stents have been used to stabilise oral anatomy during head-and-neck radiotherapy treatments for several decades and the use of these devices for the purpose of improving organ-at-risk (OAR) sparing has been increasingly reported over recent years [12,13,15,17,18]. Verrone et al described a process by which a mouth-opening intra-oral stent was designed and fabricated by a dentist in consultation with the radiation oncology treatment team, to achieve reproducible oral positioning and improved sparing of teeth, hard palate and parotid glands [17]. Similar dentist-driven techniques have been subsequently shown to result in IMRT treatment plans that achieve lower dose to OARs including oral mucosa [12,17] and reduced OAR toxicities [13], compared to IMRT treatments planned without oral stents.

Broad adoption of these stents has been restricted by the necessity of building collaborations between radiation oncology and dental treatment facilities, the challenges of scheduling the dental appointments in coordination with radiotherapy treatment planning and with reference to the treatment start date, as well as the dentist chair time and laboratory time required to produce the stents [12,15,17]. A further potential disadvantage of stents that are rigidly fixed to the teeth is the declining tolerability of the stent during and towards the end of the radiotherapy treatment, due to oral mucositis-related pain [13].

Simple non-dentist-dependent systems for fabricating oral stents have been developed within some radiotherapy facilities [19,20]. For example, Norfadilah et al [19] and Lee et al [20] have described the creation of patient-specific oral stents (called "mouthpieces" [19] or "bite blocks" [20]), by forming wax around cylindrical rods or tubes. The former group showed that a wax stent produced more reproducible oral positioning then a cylindrical tube alone [19]. By contrast, the latter group described a heat-cured acrylic stent that was moulded using the wax stent as a pattern, as a preferable alternative to using the wax stent directly [20]. While the production of usable oral stents from wax is comparatively easy [19,20], the reported disadvantages of using wax for this purpose include the potential for the wax to “distort, move, come apart, chip away or fracture over the 6-7 week course of daily treatments” [20].

Recently, studies have demonstrated alternative methods that minimise reliance on dental services, by using 3D printing techniques to fabricate intra-oral stents based on anatomical data obtained within radiation oncology facilities [15,18]. Suitable 3D printing systems are becoming increasingly accessible, for radiotherapy departments, with high-quality consumer-grade 3D printers being purchasable for under 1000 € and a substantial range of open-source software packages being available at no cost. Wilke et al proposed a method for fabricating intra-oral stents within the radiation oncology facility, using 3D printing techniques with designs derived from diagnostic CT data [15] and Liang et al have reported on the use of an external 3D printing laboratory to provide oral stents based on teeth impressions [18].

Despite the growing literature on the topic of oral positioning stents for head-and-neck radiotherapy, no previous study has reported physical measurements of the dosimetric effects of the stents. Previous studies of oral stents have demonstrated their results using OAR dose-volume metrics [12,21], example CT images [12,16,17,21] and isodoses [12,16], as well as position reproducibility measurements [16,18,19] and treatment outcomes data [13]. Physical measurements that evaluate or verify the dose distributions predicted by treatment planning system (TPS) calculations have not been reported, despite the obvious challenge of calculating head-and-neck treatment doses accurately in the presence of large air volumes [22] such as those produced by intra-oral stents [12,17,21].

This study investigated the use of 3D printing to replace a pre-existing local wax-based stent production method and thereby produce effective and robust oral stents for use in minimising dose to healthy tissues during modulated radiotherapy treatments of the tongue. As a proof-of-concept, a sample wax stent was reproduced using food-safe polylactic acid (PLA) and the suitability of the PLA stent as a substitute for the wax stent was evaluated using physical measurements in a humanoid phantom, using radiochromic film. In addition to providing an assessment of the 3D printed stent, this study aimed to demonstrate a useful measurement method by which different stent designs and materials might be evaluated in the future.

2 Method

2.1 Design and fabrication of oral positioning stents

Two sample oral positioning stents were fabricated for evaluation and comparison in this study. One stent was constructed mostly from wax, similar to the wax stent constructed around a cylindrical tube by Lee et al [19] and the other was constructed via a 3D printing method.

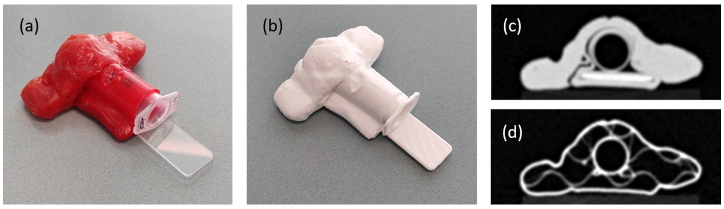

Fig. 1 Illustrations of oral positioning stents: (a) photograph of wax stent, (b) photograph of 3D printed stent, (c) transverse slice through CT image of wax stent, and (d) transverse slice through CT image of 3D printed stent.

The "wax" oral positioning stent (shown in figure 1(a)) was created manually, according to our local departmental protocol. A plastic tongue depressor was placed along the side of a plastic syringe barrel and held in place using warm wax. The syringe barrel was left open at both ends, allowing use as a breathing hole. Additional warm wax was added to the mouthpiece, to form cheek-displacing lateral wings and to achieve sufficient thickness on the anterior side of the stent to allow tooth impressions to be made, for the purpose of reproducible setup. The bulk of the stent was designed to sit behind the front teeth (which would be closed on the barrel of the stent), on the tongue, tongue-depressor side down, with the wings extending over the lower premolars/molars.

This arrangement was intended, like many oral positioning stents used locally, to simultanously separate the mandible from the maxilla, push the tongue inferiorly, away from the hard and soft palate, and push the buccal mucosa laterally, away from the tongue. The specific materials used (syringe barrel, tongue depressor and wax) were chosen in order to produce a comparatively low-density stent, which would have minimal perturbation or bolusing effects on the radiation beam, and which would also be comfortable, reproducible and robust enough for daily use over a period of several weeks. The clinical motivation for the stent design was the desire to achieve a curative radiation dose to be delivered to the tongue, while maximally sparing surrounding sensitive tissues.

In order to produce a 3D printed oral positioning stent that could be directly compared against the wax stent, the wax stent was used as the model for fabricating the 3D printed stent. The wax stent was CT scanned using a Siemens Somatom Confidence scanner (Siemens AG, Erlangen, Germany) using a tube voltage of 120 kV. To maximise the geometric resolution of the CT scan, a the field of view was reduced as much as possible and a slice thickness of 0.5 mm was used. The resulting CT image was imported into open-source 3DSlicer software [23], where the surface of the wax stent was segmented and then exported as a stereolithography file (STL) for further processing using free MeshMixer software (Autodesk Inc, San Rafael, USA). In MeshMixer, the STL file was smoothed (smothing factor 5) and repaired, to ensure that there were no gaps or non-manifold meshes in the structures, as described previously

[24]. The processed STL file was then prepared for 3D printing (converted into gcode) using Cura (Ultimaker BV, Geldermalsen, Netherlands).

The stent was 3D printed using an inexpensive consumer-grade Ender 5 3D printer (Creality 3D, Shenzhen, China), using a specific type of polylactic acid (PLA) based filament called PLA+ (3D Fillies, Dandenong South, Australia). PLA+ complies with the Australian Standard for plastics in contact with food [25] and is expected to be safe for oral use for a single patient, with sufficient cleaning or sterilisation between uses, although additional waterproofing or vapour smoothing were not investigated in this study.

The stent was printed with 0.8 mm total external wall thickness, 0.2 mm layer height, and 10% in-fill using a gyroid pattern. These settings were selected to achieve a minimum-density print, with sufficient surface smoothness to be comfortable for patient use and sufficient internal structure to be mechanically robust. The gyroid pattern was chosen (rather than one of the more commonly used grid patterns) to minimise the weight of plastic in the print while achieving a strong and isotropic internal geometry [26].

2.2 Quality assurance of oral positioning stents

After fabrication, both oral positioning stents were evaluated using visual inspection, to establish that neither stent was cracked, chipped or otherwise damaged, to verify that the breathing holes through the centre of the stents were clear from obstruction and to identify apparent external similarities and differences between the two stents. Tactile inspection was used to verify that both stents were smooth enough for use in contact with oral tissues which may be sensitive due to malignancy and can become increasingly sensitive after the commencement of radiotherapy [13]. Attempts were also made to manually compress, bend or break both oral positioning stents. These tests were repeated again after all other aspects of this study were completed.

A quantitative assessment of the geometric fidelity of the 3D printed stent was completed using an in-house 3D print quality assurance process which has been described previously [24,27,28]. Briefly, the 3D printed stent was placed on a low-density support (balsa wood block) and CT scanned using the same scanner and the same high-resolution scanning parameters as used for the wax stent (see previous section) and our in-house code was used to convert the resulting image into a STL file suitable for completing a Hausdorff distance comparison against the wax stent STL file upon which the 3D print was based, using Meshlab software [29,30].

As part of our local 3D print quality assurance process, a differential histogram of all of the Hounsfield Unit (HU) values in the CT scan of the 3D printed stent was also produced, using the in-house software [24,27,28]. For comparison, a differential HU histogram was also produced, using the CT scan of the wax mouthpiece.

2.3 Dosimetry phantom construction

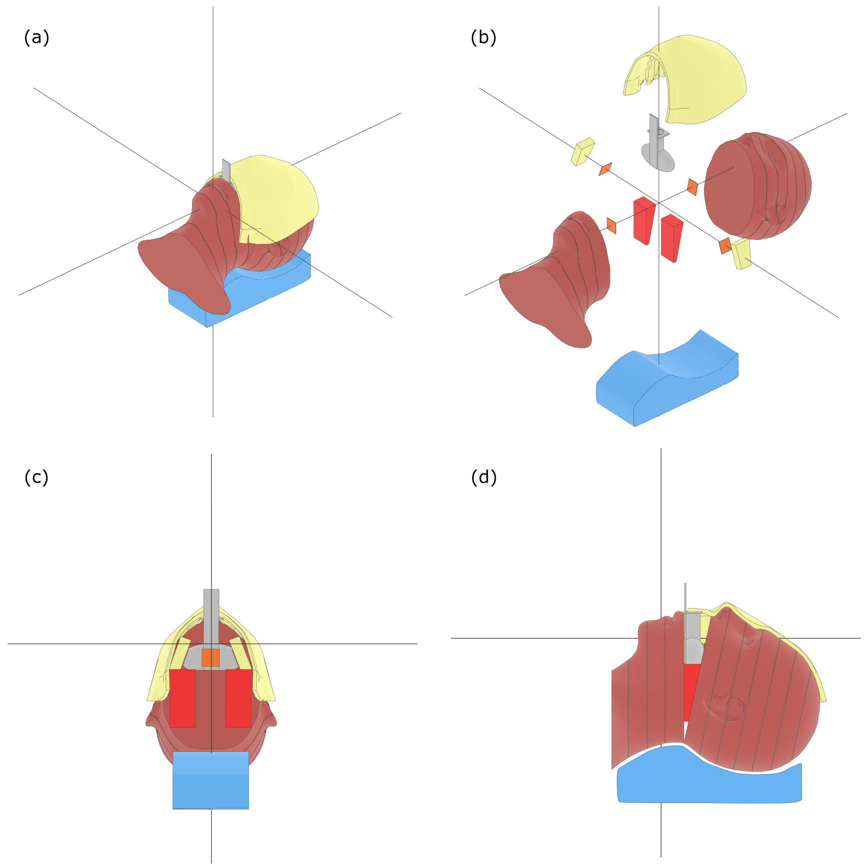

Fig. 2 Diagrams of modified head-and-neck phantom showing oral stent (grey), bolus (yellow), wax (red) and radiochromic film (orange), located in and around the phantom slices (brown): (a) isometric view; (b) exploded isometric view showing individual components; (c) transverse view through mouth; and (d) side view.

In order to evaluate the dosimetric effects of the two oral positioning stents without testing on a radiotherapy patient, it was necessary to construct a phantom with approximately realistic head-and-neck geometry and density, with an openable mouth and flexible (displaceable) cheeks. For this purpose, the head-and-neck section from a RANDO Average Man phantom (1974 model) [31] was modified as described below and shown in figures 2(a) to (d).

The 1974 RANDO Average Man phantom contains a human skeleton embedded in water-equivalent plastic with relevant air gaps (eg. oral cavity, trachea, sinuses) as well as other tissue-equivalent materials that were not used in this study (eg. lung) [31]. The phantom is divided into 2.5 cm thick transverse slices, originally designed to accommodate thermoluminescent dosimeters [31].

To achieve an open mouthed position, two phantom slices at mouth level were wedged open using 3.5 cm long wax wedges (density approx 0.9 g/cm^3). Initially, tape was wrapped around the head to support the open-mouth position. To ensure stability of the position throughout the study, the phantom was placed on a headrest and a thermoplastic shell was moulded around the posterior and lateral sides of the head. Flexible “cheeks” were created using $4 \times 2 \times 2$ cm^3 blocks of gel bolus, with the aim of achieving contact with the lateral edges of the wings on each stent. Finally, the outer cheeks and upper lip were modelled by wrapping a 0.5 cm thick sheet of Super-Flex bolus (density 1.03 g/cm^3) over the open mouth, over the nose and forehead and down the sides of the face.

During CT scanning and treatment delivery, each oral stent was positioned inside the mouth and secured using tape extending around the mouthpiece and down towards the lateral sides of the chin. Reproducibility of this positioning was achieved with reference to a marked position on the lower side of the phantom’s mouth. The positioning of radiochromic film around the stents (as suggested by figures 2(b) and (c)) is described in the next section.

2.4 Simulation and treatment planning

In order to evaluate the suitability of the oral positioning stents in terms of density and effects on surrounding simulated tissues, the modified head-and-neck phantom described in the previous section was CT scanned once with each of the two stents in place The CT scans were then used to inspect the density of the stents in relation to surrounding anatomy and observe any displacement of the flexible bolus cheeks before also being used in the planning of two different tongue radiotherapy treatments with each oral positioning stent (four treatments total).

CT scanning was performed using the same CT scanner at the same tube voltage as used to separately scan the two stents for 3D print design and quality assurance (described in previous sections). For these scans, however, the high-resolution settings (small field of view, 0.5 mm slice thickness) were replaced by a standard head-and-neck scanning protocol, with 40 cm field of view and 2 mm slice thickness, to replicate a conventional radiotherapy simulation scan. These scans were imported into the Varian Eclipse treatment planning system (Varian Medical Systems, Palo Alto, USA), version 13.7 [32], for treatment planning.

Two sample head-and-neck volumetric arc radiotherapy (VMAT) treatment plans were selected for use in this study as broadly indicative of the range of dose distributions used to treat tongue primaries; one treatment was planned for a primary only using two 160 degree VMAT arcs (avoiding posterior anatomy), and the other treatment was planned as a simultaneous integrated boost to primary plus nodes using two 360 degree VMAT arcs.

Treatment planning for this study consisted of copying each of the two sample treatment plans onto each of the two CTs of the head phantom and iteratively recalculating dose and adjusting the isocentre position, to achieve approximately realistic positioning of the high-dose region to cover the tongue and underlying muscles. All dose calculations used the Eclipse AAA algorithm and all treatments were planned for delivery using a nominal 6 MV photon beam from a Varian iX linac.

This method produced four different treatment plans: a tongue-only treatment planned for the phantom with the wax stent, a tongue-only treatment planned for the phantom with the 3D printed stent, a tongue-plus-nodes treatment planned for the phantom with the wax stent, and a tongue-plus-nodes treatment planned for the phantom with the 3D printed stent. Care was taken to ensure that two tongue-only treatments with the two different stents used the same isocentre as each other and the two tongue-plus-nodes treatments with the two different stents used the same isocentre as each other, to allow reliable comparison of the effects of the different stents.

2.5 Treatment delivery and measurement

Due to the potential confounding effects on the TPS dose calculations caused by the steep density gradients within the treated volumes of the phantom, radiochromic film measurements were used to verify the apparent effects of the different oral positioning stents on the dose to the target as well as the sensitive structures positioned by the stents.

To perform these measurements, each of the four treatments (described in the previous section) was delivered as planned, with the phantom set up to each planned isocentre position, on a Varian iX linac. The entire phantom setup remained constant from simulation through to measurement, with no parts disassembled at any time, except for the exchanging of the two different oral positioning stents and the adding and removal of small pieces of radiochromic film.

The film used was Gafchromic EBT3 film (Ashland Inc, Covington, USA), which has previously been established for measuring dose on surfaces (air-tissue interfaces) [33–36], including dose on surfaces of large internal air volumes [33].

For each treatment, four small (2.5×2.5 cm^2) pieces of film were placed inside the phantom's constructed oral cavity, at key measurement locations adjacent to the oral stent: on the top of the tongue (on the treatment target, directly inferior of the oral stent), on the roof of the mouth (measuring dose to the hard palate OAR, superior of the oral stent), inside the left and right cheeks (measuring dose to the left and right buccal mucosa OARs, directly between the ends of the lateral wings of the stent and the cheek surfaces).

The film was handled, calibrated and analysed using an established method for performing accurate dosimetry measurements using Gafchromic EBT2 and EBT3 film [36–40], including: scanning film before and after irradiation to calculate pixelwise net optical densities; making sure all film pieces were scanned at the same orientation; keeping all measurement films and calibration films together in (a light-tight box) to maintain the same thermal history; and performing the calibration irradiations within an hour of the measurement irradiations so that when the film was scanned approximately 20 hours after irradiation, the effects of different film development times were minimised.

The film was calibrated by delivering 14 different known doses ranging from 0 cGy to 344 cGy to 14 small (2.5×4.0 cm^2) pieces of film from the same sheet as the pieces used for the measurements. Since the mock prescription was 200 cGy per fraction, for both treatment plans, and the measurement involved the delivery of one fraction of each treatment to the various measurement films, the calibration range was selected to produce a calibration curve that greatly exceeded the maximum expected dose at the surface of the target, while including low-dose values suitable for accurately measuring out-of-field dose at the cheeks and palate.

3 Results

3.1 Oral positioning stent fabrication and quality assurance

Construction of the wax stent was completed in less than thirty minutes, including softening the wax in warm water, forming the stent, and then allowing ten minutes for the wax to cool and set. The 3D printed mouthpiece was successfully fabricated in 3 hours and 40 minutes, with the longest dimension standing vertical, for easy construction of the breathing hole and for achieving a successful print with a minimal area requiring support structures. Visual examination showed that both stents were complete and apparently identical (see figures 1(a) and (b)), with no obvious damage and no obstruction of the breathing aperture. Thorough tactile inspection showed that both stents were smooth, although the two stents had rows of alignment bumps on the central barrel surface that, if used in a patient treatment, would only be in contact with the teeth.

Initial attempts to manually manipulate the two stents showed that they were both sufficiently rigid and robust for use in this study. The wax stent was judged to meet our local quality standard for commencing treatment. More vigorous attempts to damage both stents after the experimental aspects of this study were completed resulted in no damage to the 3D printed stent, whereas the wax stent was easily dented using fingernail-pressure, deformed by biting and cracked by a drop onto linoleum-covered concrete floor from a height of 100 cm. The crack was sufficient to suggest that the wax stent could be destroyed by further attempts at bending, so the manual examination was stopped at this point, rather than taking this comparatively-unrealistic step.

The Hausdorff distance comparison component of our local 3D print quality assurance programme [24, 27, 28], shown in figure 3(a), indicated that a

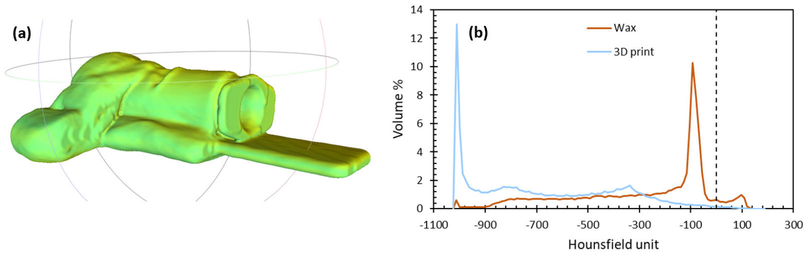

Fig. 3 (a) Visual representation of Hausdorff distance comparison with agreement within 1 mm showing as green and disagreement greater than 1 mm showing as red. (b) Differential histograms of HU values within the CT scans of wax and 3D printed stents in figures 1(c) and (d). Vertical dotted line indicates HU = 0.

majority of the external surface of the 3D printed stent matched the external surface of the wax mouthpiece on which it was based within 0.2 to 0.3 mm.

Figure 3(b) shows the differential histogram comparison of the two oral positioning stents. The wax mouthpiece results showed a large peak at approximately 100 HU and a long low-density tail, suggesting an approximate wax density of 0.9 g/cm^3, with small air gaps within the mouthpiece and volume averaging at the surface. The PLA mouthpiece showed a substantial peak at approximately 1000 HU and no peak near 0 HU, possibly due to the internal volume being largely composed of air (within the gyroid mesh, see figure 1(d)) and volume averaging on both sides of the print's internal and external walls. This result suggested that the 3D printed stent would be suitable for its intended use in supporting oral anatomy with minimal perturbation of the radiation dose delivered during the treatment.

3.2 Effects of oral positioning stent on planned dose distribution

Figures 4(a) to (d) show the dose distributions calculated by the treatment planning system for the tongue-plus-nodes treatment plan ((a) and (b)) and the tongue-only treatment plan ((c) and (d)), when the oral positioning stent used in the phantom was constructed using wax ((a) and (c)) and 3D printed from food-safe PLA+ ((b) and (d)).

Sagittal isodose distributions for both cases (figures 4(a) to (d)) show minor differences between the dose distributions calculated with the wax stent and the 3D printed stent in terms of the dose within, or on the anterior, posterior or inferior sides of the targeted tongue and underlying muscle.

For the tongue-only treatment, small differences are apparent in figures 4(c) and (d) between the level of low-dose spillage in the oral cavity, superior of the target (e.g. compare the shapes of the light-blue 10% isodose lines in these figures), with the 3D printed stent permitting slightly more transmission of this low, out-of-field dose.

As an indication of the effects of the oral stents on the positioning and out-of-field dose to the buccal mucosa, figures 5(a) to (d) show the planned

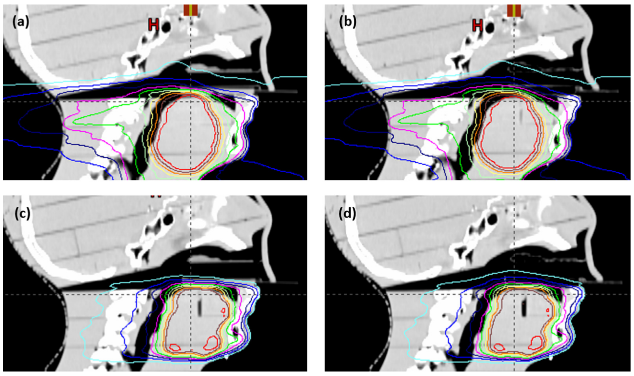

Fig. 4 Planned dose distributions (sagittal plane): (a) primary-plus-nodes treatment with wax stent, (b) primary-plus-nodes treatment with 3D printed stent, (c) primary-only treatment with wax stent, (d) primary-only treatment with 3D printed stent.

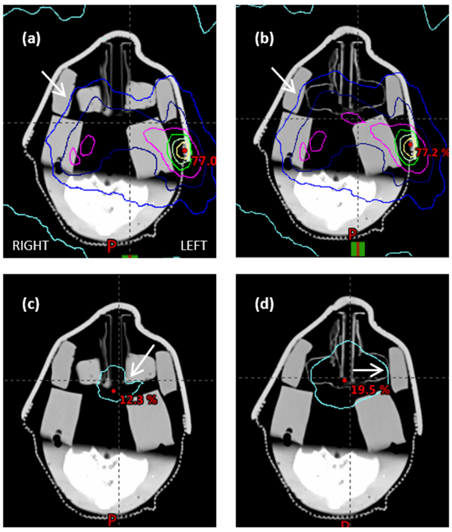

Fig. 5 Planned dose distributions (sagittal plane): (a) primary-plus-nodes treatment with wax stent, (b) primary-plus-nodes treatment with 3D printed stent, (c) primary-only treatment with wax stent, (d) primary-only treatment with 3D printed stent. The left- and right-hand sides of the phantom for all images are the same as labelled in (a). Arrows indicate features of interest, described in the text.

dose distributions in transverse planes through the open mouth, located 1.0 cm superior of the mandibular section of the phantom.

Although not clearly apparent in the CT slices shown in figures 5(a) to (d), contact between the oral positioning stents and the bolus "cheeks" was visible when scrolling through all CT volume images, confirming that both stents pushed the cheeks laterally, away from the primary target.

Comparison of the low-dose isodoses in figures 5(a) and (b) suggests that the 3D printed mouthpiece had a minimal effect on the dose to the left buccal mucosa, but slightly increased the 20% isodose coverage of the right buccal mucosa (indicated by arrows in the figure).

The area of the 10% isodose in figure 5(c), where the stent was made from wax, was similarly smaller than the area of the 10% isodose in figure 5(d), where the stent was 3D printed. This is highlighted by the the arrow in figure 5(c), which indicates a region of increased attenuation due to the wax having a much higher density than the surrounding air, and the arrow in figure 5(d), which indicates the much closer approach between the 20% isodose line and the left buccal mucosa. Note, however, that the isodoses shown both in both of these figures only cover parts of the stents and intervening air inside the open mouth, and not any relevant phantom anatomy.

3.3 Verification of dosimetric effects of oral positioning stent

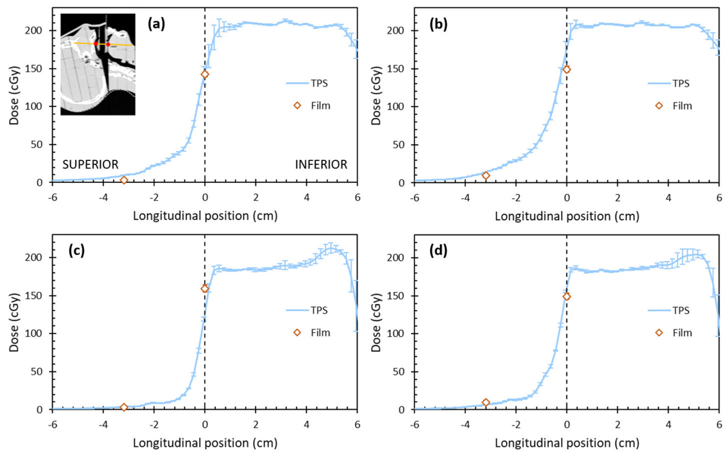

Fig. 6 TPS longitudinal dose profile vs film point dose measurements: (a) primary-plus-nodes treatment with wax stent, (b) primary-plus-nodes treatment with 3D printed stent, (c) primary-only treatment with wax stent, (d) primary-only treatment with 3D printed stent. Inset in (a) shows TPS profile location (yellow line) and film measurement locations (red dots) for all four results. Superior and inferior directions of all four profiles are the same as labelled in (a).

Figures 6(a) to (d) show the point doses measured using film on the surface of the hard palate and the top of the tongue, overlying the corresponding longitudinal dose profiles from the treatment planning system, for both treatment plans and both oral positioning stents. The planned dose profiles extend superiorly through the centre of the targeted tongue in the mandibular section of the phantom, across the oral cavity and into the maxillar section of the phantom (see inset in figure 6(a)). The film dose points were measured on the top of the tongue and on the hard palate, so that the film dose measurement points shown on each of the graphs in figure 6(a) to (d) indicate the vertical extent of the gap between mandibular and maxillar sections of the phantom.

For both treatment plans, and both stents, the dose profiles in figures 6(a) to (d) clearly show the high dose throughout the targeted tongue (on the inferior side of each profile) and the dose falloff at the mandibular edge of the oral cavity. This dose falloff is slightly less steep for the primary-only treatment plan with the 3D printed stent in figure 6(b) than for the primary-only treatment plan with the wax stent in figure 6(d).

Examination of data in figures 6(a) to (d) shows that the planned and measured dose at the surface of the hard palate, for both treatment plans and both stents, achieved the goal of minimising dose to the hard palate with a $> 90\%$ decrease in dose from the surface of the tongue to the surface of the hard palate. Evidently, both the wax stent and the 3D printed stent were successful in keeping the mouth open and displacing the hard palate from the intermediate dose region immediately superior of the tongue.

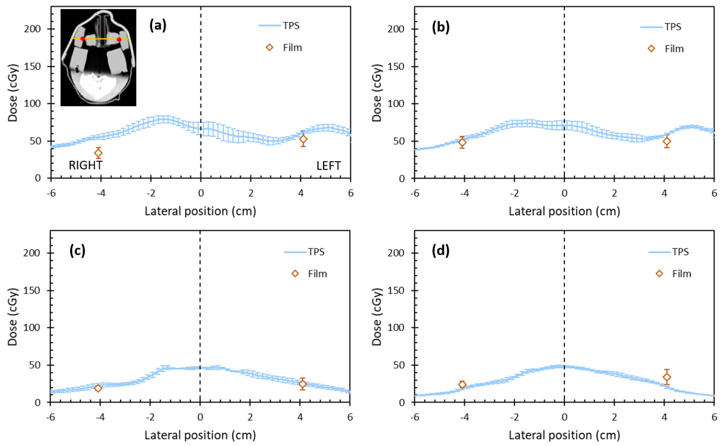

Fig. 7 TPS lateral dose profile vs film point dose measurements: (a) primary-plus-nodes treatment with wax stent, (b) primary-plus-nodes treatment with 3D printed stent, (c) primary-only treatment with wax stent, (d) primary-only treatment with 3D printed stent. Inset in (a) shows TPS profile location (yellow line) and film measurement locations (red dots) for all four results. Left and right directions of all four profiles are the same as labelled in (a).

Figures 7(a) to (d) show the point doses measured using film on the surface of the hard palate and the top of the tongue, overlying the corresponding lateral dose profiles from the treatment planning system, for both treatment plans and both oral positioning stents. In these figures, the dose profiles extend laterally through the oral cavity, superior of the treated tongue, and the film does measurement points are located on the inner surfaces of the phantom's thick bolus "cheeks".

All profiles shown in figures 7(a) to (d) show a central elevated dose, due to the proximity of the targeted tongue, with lower doses to the right and left. Some added complexity is apparent in the results for the primary-plus-nodes treatments (figures 7(a) and (b)) due to the planned intermediate dose to the jugular nodes. The film dose points show the locations of the buccal mucosa surfaces, which have been pushed into lower dose regions lateral to the tongue. The film measurement results also generally confirm the treatment planning system's calculations of the doses in these regions, with the exception of the primary-plus nodes treatment with the wax mouthpiece (figure 7(a)), where an inconsistency at the right buccal mucosa may have resulted from an unintended displacement of the film within the phantom.

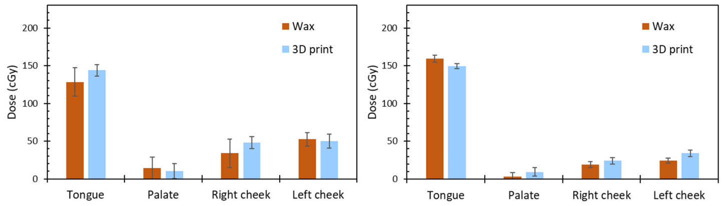

Fig. 8 Dose at "tissue" surfaces adjacent to features of the oral positioning stent, for (a) the primary-plus-nodes treatment plan and the (b) the primary-only treatment plan.

Figures 8(a) and (b) summarise the film measurement results and provide a direct comparison of the effects of the two different oral positioning stents. These figures show that generally each pair of film measurements, for the two different oral positioning stents, agreed with each other within uncertainties. The only exception was the right cheek for the primary-plus-nodes treatment plan (shown in figure 8(a)), where the film measurement adjacent to the wax stent was unusually low (compared to both the planned dose and the results for the 3D printed stent, see figures 7(a) and (b)).

The agreement between each pair of dose measurements at the hard palate, buccal mucosa (cheek) and tongue surfaces suggests that the dose differences predicted by the treatment planning system throughout the open mouth (due to the different the stent materials, see figures 5(c) and (d) and figures 5(a) to (d)) had minimal effect on the doses delivered to surrounding tissues.

4 Discussion

This study evaluated the use of 3D printed oral positioning stent as a potential replacement for the use of wax positioning stents that have been described previously [19, 20] and are used locally, in our radiotherapy department. Whereas previous investigations of the use of oral positioning stents for head-and-neck radiotherapy treatments have reported results using CT images and planned dose calculations for human patients [12, 16, 17, 21], this study used a modified head phantom to perform physical dose measurements to investigate the accuracy of treatment planning system dose calculations for sensitive tissues adjacent to the stents.

The use of a phantom, rather than a human patient or volunteer, was clearly the major limitation of this study. Although modified using gel boluses, the phantom was unable to replicate the flexibility and elasticity of important oral structures such as the cheeks and the tongue. For example, results shown in figures 6(a) to (d) suggest the potential for the oral positioning stents to depress the tongue down and away from the sensitive tissues of the hard and soft palate, but this could not be demonstrated practically due to phantom not having either a flexible tongue or a space where a flexible (eg. gel) tongue could be placed.

A further limitation was the inherently limited reproducibility of the specific phantom used, and especially its inaccessible teeth (embedded in plastic). For a standard patient treatment, the wax stent can be formed to fit the teeth to achieve reproducible positioning, similar to a bite block. A more sophisticated, purpose built phantom with accessible teeth, a movable tongue, and the ability to open and close the jaw would be an ideal solution. 3D printing is a potential method for the development of this ideal phantom solution in the future.

The use of the modified RANDO phantom for this work, however, had the key advantages of allowing CT imaging and VMAT treatments to be repeated, with different stents in the same setup, and allowing radiochromic film measurements of dose inside the mouth to be performed within minimal uncertainty.

The restriction of this study to two treatment plans for one anatomical site was an additional limitation of this study. Tongue treatments were chosen as the focus of this study due to the long-established role or oral positioning stents in treatments of the tongue, in particular [21]. Two tongue different treatment plans, one including a simultaneous integrated boost to nodes and the other treating the primary only, were used to provide an indication of the range of out-of-field dose distributions that might be encountered when using oral positioning stents. However, further studies with different treatment sites and dose distributions are advisable, as part of any 3D printed oral stent adoption process.

The major difference between the primary-plus-nodes treatment plan and the primary-only treatment plan used in this study is most obvious when comparing the transverse planes in figures 5(a) and (c) or figures 5 (b) and (d). Whereas the primary-only treatment in figures 5(c) and (d) shows a localised region of comparatively low-dose spillage from the primary target into the open mouth, the primary-plus-nodes treatment (figures 5(a) and (b)) includes large areas of intermediate dose located laterally and posteriorly of the primary target, intended to cover the jugular nodes.

Another subtler difference between the results for the two different treatment plans is the comparatively increased low-dose spillage into oral cavity, for primary-only treatment, when the 3D printed stent is used. The effect was not apparent in the results for the primary-plus-nodes treatment plan, where the dose throughout the oral cavity was generally higher due to planned dose to adjacent node regions.

For the primary-only treatment plan, the isodose distributions in figures 4(d) and 5(d) both show increased an increased coverage by the 10% isodose within the oral cavity, superior to the tongue, which is also apparent in the shallower gradient of the dose falloff shown in figure 6(d) compared to figure 6(d). The increased volume of low out-of-field dose spillage seen when the primary-only treatment was applied to the phantom with the 3D printed stent can be attributed to the reduced attenuation (reduced beam perturbation) through the low-density 3D printed stent, compared to the wax. In this case, figures 4(d) and 6(d) also show that the effects of this reduced perturbation were localised close to the mandibular edge of the oral cavity, with minimal effects on the dose to the hard palate.

This effect, keeping the sensitive hard palate away from the high dose delivered to the tongue, while simultaneously pushing the buccal mucosa out of the intermediate dose region in the oral cavity, was apparent for both treatment plans (despite the differences described above) and both oral positioning stents (despite their internal differences in density and structure, shown in figures 1(c) and (d)). A collation of results from the film measurements and planned dose profiles demonstrated the cheek displacement and mouth opening ability of both stents. Data in figures 7(a) to (d) and figures 6(a) to (d)) show that the film measurement results were generally in agreement with the planned doses at the corresponding points, in challenging density-interface regions on the tongue, palate, and buccal mucosa surfaces.

The agreement between the doses measured at the surface of the tongue and OARs for the two different oral positioning stents, shown for the primary-plus-nodes treatment in figure 8(a) and for the primary-only treatment in figure 8(b), suggests that the change of stent material and density had no detrimental effect on the dose to target or the sparing of the OARs, from either treatment plan. The additional, non-dosimetric testing of the two oral positioning stents, which included visual and tactile inspection and manual manipulation, as well as routine 3D print quality assurance, indicated that the 3D print accurately replicated the external geometry of the wax stent, including a suitably smooth surface for clinical use. These tests also showed that the 3D printed stent was physically more robust than the wax stent, despite having a lower internal density.

The stability and reproducibility of the oral positioning stent are essential, if the stent is to be used for accurate and safe radiation treatment delivery. The results of the physical testing of the two stents suggested that the robustness of food safe PLA+ was superior to wax. In local clinical use, wax stents have been observed to lose integrity with repeated use over the course of treatment, leading to pieces of wax detaching and potentially becoming hazardous to supine patients due to the risk of choking.

Overall, the results of this study suggest that 3D printed oral positioning stents can be designed to be more physically robust while having reduced effects on the radiation treatment beam, compared to the wax stents that they are intended to replace. These effects are dependent on the infill density of each print. For example, in this study the goal was to achieve minimal beam perturbation, but it should also be possible to optimise infill density to replicate the attenuation effects caused by wax, or achieve other deliberate beam perturbations (such as shielding [41]) if desired. Future work in this area could also involve investigations into pre-printed modular systems, to minimise the number or duration of patient appointments for stent preparation.

5 Conclusion

This study confirmed the potential utility of using 3D printed oral positioning stents to facilitate the accurate and reproducible delivery of head-and-neck radiotherapy treatments. Treatment plan dose calculations and film measurements demonstrated that a 3D printed stent was able to achieve the same degree of displacement of OAR tissue away from the intermediate dose region, and therefore achieve the same reduced doses to relevant OARs, as a wax stent. The film measurements also showed negligible effect on the dose to the target (tongue) when a wax stent was substituted for a 3D printed stent.

The results of this study suggest that the adoption of a 3D printing process for stent fabrication has the potential to achieve stable and reproducible positioning of the cheeks, lips and tongue during head-and-neck radiotherapy, while also eliminating the hazards posed by wax stents losing their physical integrity.

Further work in this area could involve investigations of the use of 3D printed stents for treatments of other targets in the head-and-neck region, or investigations of alternative 3D printing materials and designs, including pre-printed modular systems.

The dosimetric investigation methods, including film dosimetry measurements, demonstrated in this study are expected to enable future investigations into different applications, designs or materials for 3D printed oral positioning stents with minimal need for patient testing, especially if more sophisticated phantoms (with appropriately flexible oral structures) can also be fabricated using 3D printing or other techniques.

Delarations

Funding: Contributions to this work from Susannah Cleland, Scott B. Crowe, Elise Obereigner and Tania Tutaki were supported by a Metro North Hospital and Health Service funded Herston Biofabrication Institute Programme Grant (no grant number).
Conflict of Interest: All authors declare that they have no conflicts of interest.
Ethical approval: This article does not contain any studies with human participants performed by any of the authors.

References

1. Parliament, M.B., Scrimger, R.A., Anderson, S.G., Kurien, E.C., Thompson, H.K., Field, G.C. and Hanson, J., 2004. Preservation of oral health–related quality of life and salivary flow rates after inverse-planned intensity-modulated radiotherapy (IMRT) for head-and-neck cancer. Int J Radiat Oncol Biol Phys 58(3): 663-673.
2. Navran, A., Heemsbergen, W., Janssen, T., Hamming-Vrieze, O., Jonker, M., Zuur, C., Verheij, M., Remeijer, P., Sonke, J.J., van den Brekel, M. and Al-Mamgani, A., 2019. The impact of margin reduction on outcome and toxicity in head and neck cancer patients treated with image-guided volumetric modulated arc therapy (VMAT). Radiother Oncol 130: 25-31.
3. Johnston, M., Clifford, S., Bromley, R., Back, M., Oliver, L. and Eade, T., 2011. Volumetric-modulated arc therapy in head and neck radiotherapy: a planning comparison using simultaneous integrated boost for nasopharynx and oropharynx carcinoma. Clin Oncol 23(8): 503-511.
4. Holt, A., Van Gestel, D., Arends, M.P., Korevaar, E.W., Schuring, D., Kunze-Busch, M.C., Louwe, R.J. and van Vliet-Vroegindeweij, C., 2013. Multi-institutional comparison of volumetric modulated arc therapy vs. intensity-modulated radiation therapy for head-and-neck cancer: a planning study. Radiat Oncol 8: 26.
5. Stieler, F., Wolff, D., Schmid, H., Welzel, G., Wenz, F. and Lohr, F., 2011. A comparison of several modulated radiotherapy techniques for head and neck cancer and dosimetric validation of VMAT. Radiother Oncol 101(3): 388-393.
6. Osborn, J., 2017. Is VMAT beneficial for patients undergoing radiotherapy to the head and neck?. Radiogr 23(1): 73-76.
7. Lin, C.G., Xu, S.K., Yao, W.Y., Wu, Y.Q., Fang, J.L. and Wu, V.W., 2017. Comparison of set up accuracy among three common immobilisation systems for intensity modulated radiotherapy of nasopharyngeal carcinoma patients. J Med Radiat Sci 64(2): 106-113.
8. Hansen, C.R., Christiansen, R.L., Nielsen, T.B., Bertelsen, A.S., Johansen, J. and Brink, C., 2014. Comparison of three immobilisation systems for radiation therapy in head and neck cancer. Acta Oncol 53(3): 423-427.
9. Leech, M., Coffey, M., Mast, M., Moura, F., Osztavics, A., Pasini, D. and Vaandering, A., 2017. ESTRO ACROP guidelines for positioning, immobilisation and position verification of head and neck patients for radiation therapists. Tech Innov Patient Support Radiat Oncol 1: 1-7.
10. Gilbeau, L., Octave-Prignot, M., Loncol, T., Renard, L., Scalliet, P. and Grégoire, V., 2001. Comparison of setup accuracy of three different thermoplastic masks for the treatment of brain and head and neck tumors. Radiother Oncol 58(2): 155-162.
11. Sharp, L., Lewin, F., Johansson, H., Payne, D., Gerhardsson, A. and Rutqvist, L.E., 2005. Randomized trial on two types of thermoplastic masks for patient immobilization during radiation therapy for head-and-neck cancer. Int J Radiat Oncol Biol Phys 61(1): 250-256.
12. Grant, S.R., Williamson, T.D., Stieb, S., Shah, S.J., Fuller, C.D., Rosenthal, D.I., Frank, S.J., Garden, A.S., Morrison, W.H., Phan, J., Moreno, A.C., 2020. A dosimetric comparison of oral cavity sparing in the unilateral treatment of early stage tonsil cancer: IMRT, IMPT, and tongue deviating oral stents. Adv Radiat Oncol 5(6): 1359-1363
13. Stieb, S., Perez Martinez, I., Mohamed, A.S., Rock, S., Bajaj, N., Deshpande, T.S., Zaid, M., Garden, A.S., Goepfert, R.P., Cardoso, R., Ferrarotto, R., 2020. The impact of tongue deviating and tongue depressing oral stents on long term radiation associated symptoms in oropharyngeal cancer survivors. Clin Transl Radiat Oncol 24: 71-78.
14. Hong, C.S., Oh, D., Ju, S.G., Ahn, Y.C., Na, C.H., Kwon, D.Y., Kim, C.C., 2019 Development of a semi customized tongue displacement device using a 3D printer for head and neck IMRT. Radiat Oncol 14: 79.
15. Wilke, C.T., Zaid, M., Chung, C., Fuller, C.D., Mohamed, A.S., Skinner, H., Phan, J., Gunn, G.B., Morrison, W.H., Garden, A.S., Frank, S.J., 2017. Design and fabrication of a 3D printed oral stent for head and neck radiotherapy from routine diagnostic imaging. 3D Print Med 3: 12.
16. Doi, H., Tanooka, M., Ishida, T., Moridera, K., Ichimiya, K., Tarutani, K., Kitajima, K., Fujiwara, M., Kishimoto, H. and Kamikonya, N., 2017. Utility of intraoral stents in

external beam radiotherapy for head and neck cancer. Rep Pract Oncol Radiother 22(4): 310-318.
17. Johnson, B., Sales, L., Winston, A., Liao, J., Laramore, G., Parvathaneni, U., 2013. Fabrication of customized tongue displacing stents: considerations for use in patients receiving head and neck radiotherapy. J Am Dent Assoc 144(6): 594-600.
18. Liang, R., Lehnhardt, J., Chang, C., Roberts, G., Gaudilliere, D., Hara, W., Le, Q.T., Beadle, B.M., 2018. Use of 3D printed custom oral stents to improve positioning and reproducibility for patients treated for head and neck cancer. Int J Radiat Oncol Biol Phys 102(3): e329-e330.
19. Norfadilah, M.N., Ahmad, R., Heng, S.P., Lam, K.S., Radzi, A.B. and John, L.S.H., 2017. Immobilisation precision in VMAT for oral cancer patients. J Phys Conf Ser 851: 012025.
20. Lee, V.S.K., Nguyen, C.T. and Wu, J., 2019. The fabrication of an acrylic repositioning stent for use during intensity modulated radiation therapy: a feasibility study. J Prosthodont 28(6): 643-648.
21. Verrone, J.R., Alves, F.D.A., Prado, J.D., Boccaletti, K.W., Sereno, M.P., Silva, M.L.G. and Jaguar, G.C., 2013. Impact of intraoral stent on the side effects of radiotherapy for oral cancer. Head Neck 35(7): E213-E217.
22. Crowe, S.B., Kairn, T., Trapp, J.V., Fielding, A.L., 2013. Monte Carlo evaluation of collapsed-cone convolution calculations in head and neck radiotherapy treatment plans. IFMBE Proc 39: 1803-1806. https://doi.org/10.1007/978-3-642-29305-4_474
23. Fedorov, A., Beichel, R., Kalpathy-Cramer, J., et al, 2012. 3D Slicer as an Image Computing Platform for the Quantitative Imaging Network. Magn Reson Imaging 30(9): 1323-1341.
24. Kairn, T., Zahrani, M., Cassim, N., Livingstone, A.G., Charles, P.H., Crowe, S.B., 2020. Quasi simultaneous 3D printing of muscle-, lung- and bone-equivalent media: a proof of concept study. Phys Eng Sci Med 43(2):701-710.
25. Standards Australia, Plastic materials for food contact use, AS 2070-1999 (1999)
26. Tino, R., Leary, M., Yeo, A., Brandt, M. and Kron, T., 2019. Gyroid structures for 3D-printed heterogeneous radiotherapy phantoms. Phys Med Biol 64(21): 21NT05.
27. Charles, P.H., Kairn, T., Crowe, S.B., 2020. Clinical quality assurance of 3D printed patient specifc radiotherapy devices. Phys Eng Sci Med 43(1):436–437. https://doi.org/10.1007/s13246-019-00826-6. Correction to: EPSM 2019, Engineering and Physical Sciences in Medicine. Phys Eng Sci Med 43(1):463 (2020). https://doi.org/10.1007/s13246-020-00846-7
28. Sasaki, D.K., McGeachy, P., Aviles, J.E.A., et al, 2019. A modern mold room: Meshing 3D surface scanning, digital design, and 3D printing with bolus fabrication. J Appl Clin Med Phys 20(9): 78-85.
29. Cignoni, P., Callieri, M., Corsini, M., et al, 2008. MeshLab: an Open-Source Mesh Processing Tool, Sixth Eurographics Italian Chapter Conference, 129-136.
30. Cignoni, P., Rocchini, C., Scopigno, R., 1998. Metro: measuring error on simplified surfaces, Comput Graph Forum 17(2): 167-174.
31. Alderson, S.W., Lanzl, L.H., Rollins, M., Spira, J., 1962. An instrumented phantom system for analog computation of treatment plans. Am J Roentgenol Radium Ther Nucl Med 87: 185-195.
32. Binny, D., Kairn, T., Lancaster, C.M., Trapp, J.V., Crowe, S.B., 2018. Photon Optimizer (PO) versus Progressive Resolution Optimizer (PRO): A conformality and complexity based comparison for Intensity Modulated Arc Therapy plans. Med Dosim 43(3): 267-275.
33. Kairn, T., Lathouras, M., Grogan, M., Green, B., Sylvander, S.R., Crowe, S.B., 2021. Effects of gas filled temporary breast tissue expanders on radiation dose from modulated rotational photon beams. Med Dosim (in press) https://doi.org/10.1016/j.meddos.2020.06.003
34. Rijken, J., Kairn, T., Crowe, S., Muñoz, L., Trapp, J., 2018. A simple method to account for skin dose enhancement during treatment planning of VMAT treatments of patients in contact with immobilisation equipment J Appl Clin Med Phys 19(4): 239-245.
35. Morales, J.E., Hill, R., Crowe, S.B., Kairn, T., Trapp, J.V., 2014. A comparison of surface doses for very small field size x-ray beams: Monte Carlo calculations and radiochromic film measurements. Australas Phys Eng Sci Med 37(2): 303-309.

36. Moylan, R., Aland, T., Kairn, T., 2013. Dosimetric accuracy of Gafchromic EBT2 and EBT3 film for in vivo dosimetry. Australas Phys Eng Sci Med 36(3): 331-337.
37. Kairn, T., Aland, T., Kenny, J., 2010. Local heterogeneities in early batches of EBT2 film: A suggested solution. Phys Med Biol 55(15): L37-L42.
38. Aland, T., Kairn, T., Kenny, J., 2011. Evaluation of a Gafchromic EBT2 film dosimetry system for radiotherapy quality assurance. Australas Phys Eng Sci Med 34(2): 251-260.
39. Kairn, T., Hardcastle, N., Kenny, J., Meldrum, R., Tome, W., Aland, T., 2011. EBT2 radiochromic film for quality assurance of complex IMRT treatments of the prostate: Micro collimated IMRT, RapidArc, and TomoTherapy. Australas Phys Eng Sci Med 34(3): 333-343.
40. Spelleken, E., Crowe, S.B., Sutherland, B., Challens, C., Kairn, T., 2018. Accuracy and efficiency of published film dosimetry techniques using a flat bed scanner and EBT3 film. Australas Phys Eng Sci Med 41(1): 117-128.
41. Crowe, S.B., Charles, P.H., Cassim, N., Maxwell, S.K., Sylvander, S.R., Smith, J.G. and Kairn, T., 2021. Predicting the required thickness of custom shielding materials in kilovoltage radiotherapy beams. Physica Medica 81: 94-101.